High-quality epitaxial growth of γ-alumina films on α-alumina sapphire induced by ion-beam bombardment

Ning Yu, Paul C. McIntyre, Michael Nastasi, and Kurt E. Sickafus
Materials Science and Technology Division, Los Alamos National Laboratory, Los Alamos, New Mexico 87545
(Received 11 September 1995)

We report the formation of epitaxial γ-alumina thin films on α-alumina substrates induced by ion-beam bombardment. Single-crystal (0001) α-alumina was coated with 70-nm amorphous-alumina thin films and then bombarded with either 360-keV argon ions or 180-keV oxygen ions at 400, 500, and 600 °C. Ion-channeling measurements showed a consistent minimum yield of 50% for the aluminum in the grown films. Cross-sectional transmission-electron microscopy revealed the formation of γ-alumina epitaxially grown onto α-alumina with an orientation relationship $[1\bar{1}0](111)\gamma \| [01\bar{1}0](0001)\alpha$. The epitaxy of γ-alumina was further confirmed by x-ray-diffraction ϕ scans. This study indicates that ion-beam bombardment at 400–600 °C not only induces the amorphous-to-γ phase transformation but also effectively eliminates $\{111\}$ twins of γ-alumina, which are normally observed after thermal annealing at 800–900 °C.

I. INTRODUCTION

Alumina (Al_2O_3) is a technologically important ceramic for structural, microelectronic, and optical applications. Previous thermal annealing studies[1] have shown that amorphous alumina transforms through metastable phases into a thermally stable α phase (hexagonal structure). The dominant intermediate metastable phase is γ-alumina (cubic structure). For the structure of an amorphous-alumina thin film on a single-crystal α-alumina (sapphire) substrate, alumina/sapphire, the amorphous phase first transforms into the γ phase and then into the α phase.[2–5] Both transformations appear to be epitaxially related to underlying sapphire following a layer-by-layer growth habit. The amorphous-to-γ transition occurs at measurable rates in the temperature range 650–900 °C and is characterized by a thermal activation energy of 3.6 eV.[3] The γ-to-α transformation occurs above 800 °C with a characteristic activation energy of 5.0 eV, as measured along the c axis ([0001]).[3,4] The intermediate γ-alumina films always appear to be defective, containing many twins, while the subsequently grown α-alumina films have fewer crystallographic defects.[2,5]

The main motivation for this study is to understand the phase transformations that occur in thin-film amorphous alumina under ion-beam bombardment at temperatures much lower than those for thermal annealing. The study of Ohkubo and Seno[6] suggested that under radiation-damage conditions using 400-keV gold ions, a reverse transformation sequence occurred in sapphire, i.e., α to γ and then γ to amorphous. Cao *et al.* also reported the conversion of α to γ by rapid melting and resolidification using a XeCl excimer laser to irradiate sapphire.[7] A question arises: Does the observed phase sequence of amorphous-γ-α occur for the alumina/sapphire under ion-beam bombardment that favors epitaxial growth? It has been demonstrated that the phase transformation between amorphous and crystalline Si is reversible by ion irradiation and that the irradiation conditions determine the transformation direction.[8] Only limited studies have been performed to investigate ion-beam-induced transition phenomena in alumina. Zhou *et al.*[9] observed ion-beam-induced epitaxial growth (IBIEG) at 400 °C in the alumina/sapphire system, where the amorphous-alumina layer was formed by In ion implantation at cryogenic temperatures. A recent study[10] further showed that IBIEG occurred at 400–600 °C in amorphous-alumina films deposited onto sapphire. However, the phase-transformation sequence resulting from ion-beam bombardment was not identified by these studies. In this work, we demonstrate that ion-beam bombardment at 400–600 °C not only induces the amorphous-to-γ phase transformation, but also eliminates twin boundaries in the γ-alumina, which are always present after thermal annealing alone at 800–900 °C.[2,5]

II. EXPERIMENT

Single-crystal (0001) sapphire substrates with one side polished to an optical finish were used for all experiments. Amorphous-alumina thin films (a-Al_2O_3) were deposited at room temperature onto the as-received substrates by electron-beam evaporation from a high-purity alumina target.[5] The amorphous nature of the as-deposited films was confirmed by transmission electron diffraction.[5] Two sets of samples with film thickness of 70 and 200 nm were produced for this study. The samples with thinner films were used for ion-beam irradiation studies to ensure the implanted ions penetrated through the films. To understand radiation effects on epitaxial growth, both 360-keV Ar^{2+} and 180-keV O^+ ion beams were chosen to irradiate the samples at the following temperatures: 400, 500, and 600 °C. The sample normal was tilted to 10° with respect to ion beams during the irradiations. The projected ranges of Ar and O ions in sapphire determined by TRIM (Ref. 11) are 215 and 226 nm, respectively, much greater than the thickness of thin film (70 nm). The fluxes of Ar and O ion beams were maintained at 1.5×10^{13} and 4.6×10^{13} atoms/cm^2 s, respectively. For comparison, samples deposited with a 70- or 200-nm alumina film were annealed at 800 °C for 1 h in flowing oxygen gas. Rutherford backscattering spectrometry and ion channeling using a 2-MeV He^+ ion beam were used to characterize the crystallinity of the alumina films on the sapphire substrates. Phase transformations and microstructure were examined by

0163-1829/95/52(24)/17518(5)/$06.00 © 1995 The American Physical Society

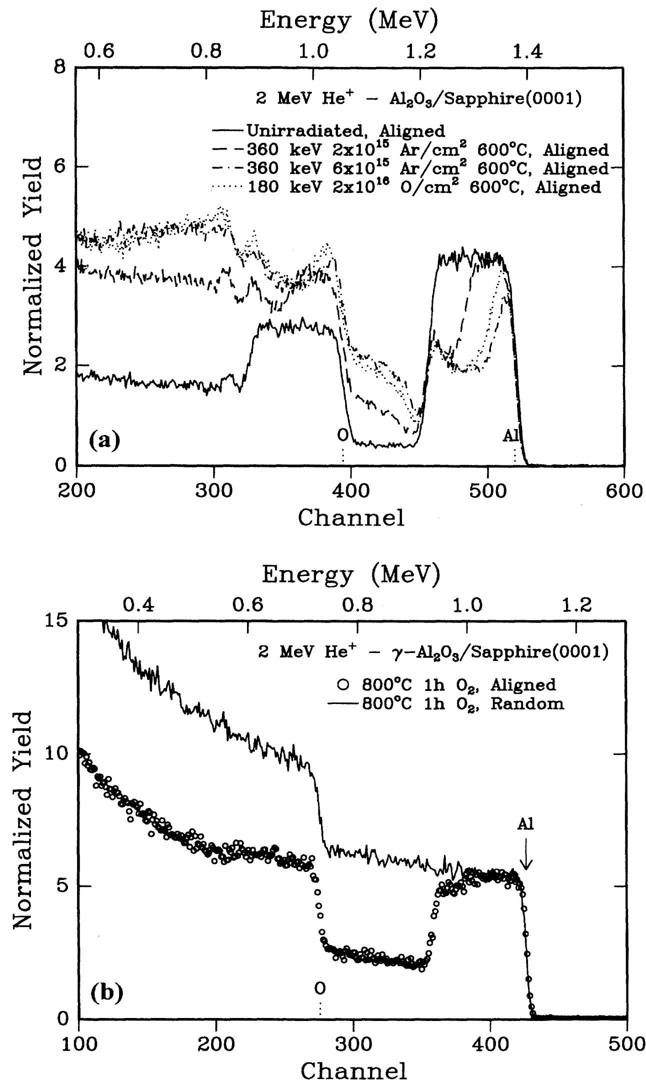

FIG. 1. Aligned backscattering spectra of the alumina/sapphire samples before and after (a) ion-beam bombardment of 360-keV Ar or 180-keV O at 600 °C; (b) thermal annealing at 800 °C for 1 h in flowing oxygen.

cross-sectional transmission electron microscopy (XTEM). The nature of the in-plane film alignment was also determined using x-ray diffraction.

III. RESULTS

Figure 1(a) shows aligned backscattering spectra of the alumina/sapphire samples before and after ion-beam bombardment with 360-keV Ar or 180-keV O at 600 °C. Both the Al and O signals indicate that epitaxial crystallization proceeded layer by layer in the film following the 360-keV Ar ion irradiation. The channeling spectra also show that the epitaxial growth slowed down near the surface as the dose increased from 2×10^{15} to 6×10^{15} Ar/cm^2. An increase in the dechanneling yield near the film surface (<20 nm) is due to its polycrystalline nature, as confirmed by TEM. Minimum yield ($X_{\rm min}$), defined as a ratio of channeling to random yield, is determined to be about 50% for Al in the epitaxially grown film. The radiation-induced lattice damage in the sub-

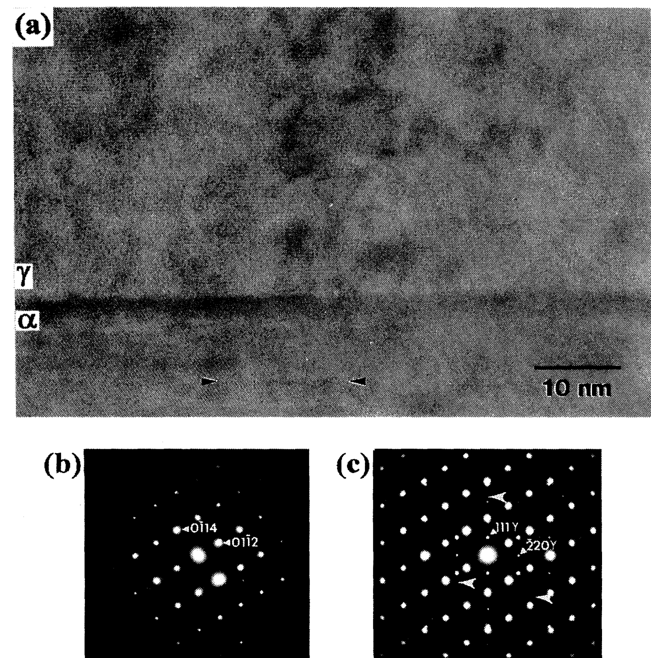

FIG. 2. (a) XTEM bright field image of the epitaxial γ-alumina/α-alumina interface; (b) SAD pattern of the α-alumina substrate; and (c) SAD pattern of both the film and substrate after irradiation with 180-keV, 6×10^{16} O/cm^2 at 500 °C.

strate region is visible as an increase in dechanneling in Fig. 1(a). Epitaxial growth is also observed in the sample irradiated with 180-keV O ions as shown in Fig. 1(a). However, to grow a similar thickness epitaxial layer, the required dose (2×10^{16} O/cm^2) for O ions is three times as high as that (6×10^{15} Ar/cm^2) for Ar ions. TRIM calculations[11] indicate that the ratio of nuclear energy loss in the film for Ar versus O irradiations is about 3.6, while the corresponding electronic energy-loss ratio is 1.6. Therefore, it appears that the higher efficiency observed for epitaxial crystallization induced by Ar ions is due to the higher nuclear energy loss of Ar ions in the alumina films. This suggests that radiation-induced defects due to nuclear energy-loss processes drive the epitaxial crystallization of amorphous alumina. Similar minimum yields (50%) were obtained from films that were crystallized under irradiation at lower temperatures, 400 and 500 °C, although the crystallization became slower compared to the films irradiated at 600 °C. In contrast, thermal annealing alone at a higher temperature (800 °C for 1 h) resulted in much poorer epitaxy during crystallization, as shown in Fig. 1(b). An average $X_{\rm min}$ value of 90% is obtained in the thermally annealed film.

Figure 2(a) is a high-resolution micrograph showing the film/substrate interfacial region after irradiation with 180-keV oxygen ions to a dose of 6×10^{16} O/cm^2 at 500 °C. The selected area electron diffraction (SAD) pattern in Fig. 2(b) was taken from the substrate area and viewed near the α-alumina $[1\bar{2}10]$ zone axis. Figure 2(c) is a SAD pattern for the film and the film/substrate interfacial region, including the area shown in Fig. 2(a). Diffracted beams present in Fig. 2(c) and not present in Fig. 2(b) are due to diffraction from the film. Most of the additional reflections in Fig. 2(c)

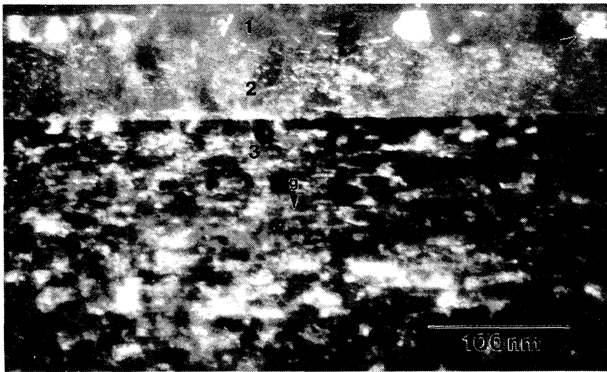

FIG. 3. XTEM weak beam image of the same specimen shown in Fig. 2; $g_{\rm film}=[222]$ and $g_{\rm subs}=[0006]$.

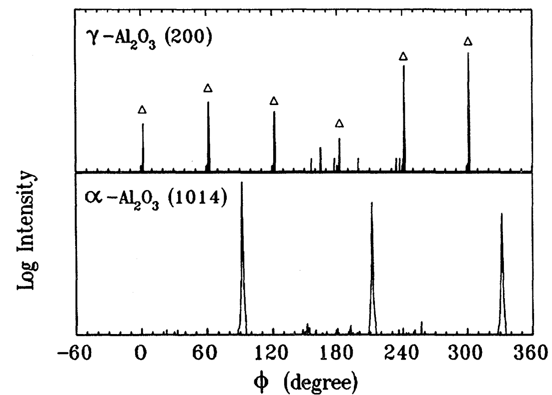

FIG. 4. X-ray-diffraction ϕ scans from the $\{10\bar{1}4\}$ α-alumina and $\{200\}$ γ-alumina planes, showing the in-plane alignment of the epitaxial (111)-oriented γ-alumina film on the (0001) α-alumina substrate, following the irradiation with 180-keV, 3×10^{16} O/cm^2 at 500 °C.

can be indexed as epitaxial γ-alumina, viewed near a $[11\bar{2}]$ zone axis. The orientation relationship between the epitaxial γ-alumina and α-alumina substrate is $[11\bar{2}](111)\gamma\|[1\bar{2}10](0001)\alpha$ or $[1\bar{1}0](111)\gamma\|[01\bar{1}0](0001)\alpha$ equivalent. The electron diffraction measurements also indicate that the sapphire substrate and the γ-alumina film have their bulk lattice parameters: $a_{(0003)\alpha}=0.433$ nm and $a_{(111)\gamma}=0.456$ nm; thus, the film is incoherent. Several weak reflections present in Fig. 2(c) (marked by large, white arrows) result from a small portion of nonepitaxial γ-alumina present near the sample surface, as indicated by the channeling data in Fig. 1(a). Numerous dislocations are present in both the film and the substrate following IBIEG. Crystallographic disorder in the γ-alumina is responsible for the mottled contrast visible in the film region. In addition, a dislocation loop on the basal plane of the α-alumina substrate is marked by arrows in the figure.

The weak beam cross-sectional image in Fig. 3 was taken with a [0006] diffraction vector for the sapphire substrate and a [222] diffraction vector for the epitaxial γ-alumina. The proximity of the film and substrate diffracted beams made it difficult to select only a film or substrate reflection with the TEM's smallest objective aperture. Figure 3 is a lower-magnification image than Fig. 2(a) and shows the two microstructural regions of the γ-alumina film: the epitaxial zone near the substrate (labeled "2" in the image) and the polycrystalline zone near the surface (labeled "1"). The epitaxial and polycrystalline zones are approximately 60 and 20 nm in thickness, respectively, consistent with the channeling measurements. Several equiaxed crystallites are in contrast in the polycrystalline zone, and these appear to span the entire thickness of this zone. Moiré fringes are clearly visible in one crystallite that is marked with an arrow. A high density of short, segmented dislocations are visible under these diffraction conditions in the epitaxial zone in Fig. 3. The orientation of the defects appears random throughout much of the expitaxial zone; however, several (111) dislocation loops with a Burgers vector having a component parallel to [111] are present near the center of the zone. A large number of basal plane loops are visible in the sapphire substrate (labeled "3" in the image). Condensation of interstitials into both $\frac{1}{3}$ [0001] (0001) and $\frac{1}{3}\langle 10\bar{1}0\rangle$ $\{10\bar{1}0\}$ four-layer loops is a common effect of ion irradiation in α-alumina.[12] Only the basal plane loop population is visible under the diffraction conditions used in Fig. 3.

A high density of {111} twins with an average boundary spacing less than 100 nm along the film/substrate interface was observed in thermally grown γ-alumina films (not shown). These twins are not observed in XTEM characterization of the ion-irradiated films over a TEM viewing range greater than 10 μm along the interface.

The same in-plane alignment of the epitaxial γ-alumina film observed in the XTEM studies was also observed in x-ray-diffraction ϕ scans. Figure 4 shows ϕ scans from a sample with a 45-nm epitaxial γ-alumina layer in a film of 70 nm total thickness, following the irradiation with 180-keV, 3×10^{16} O/cm^2 at 500 °C. Three strong $\{10\bar{1}4\}$ α-alumina peaks separated by 120° are present in the ϕ scan in Fig. 4. Six weak {200} γ-alumina film reflections were detected with 60° mutual separations. The 30° separation in ϕ of adjacent $\{10\bar{1}4\}$ α-alumina and {200} γ-alumina reflections is consistent with a $[1\bar{1}0](111)\gamma\|[01\bar{1}0](0001)\alpha$ orientation relationship. The presence of six {200} γ-alumina reflections in Fig. 4, instead of three, indicates that two types of twin domains exist within the epitaxial layer. These domains must be textured with each other at a 180° rotation angle along the [111] axis due to the existence of two sets of possible stacking sequences on the (0001) sapphire surface. The full width at half maximum intensity of the {200} γ-alumina peaks is $\sim1.4°$, compared to $\sim1.0°$ for the $\{10\bar{1}4)$ α-alumina peaks.

IV. DISCUSSION

The diffraction data clearly show that the ion beam induces an amorphous-to-γ phase transformation. An activation energy of 0.23 ± 0.05 eV (Ref. 10) was obtained from this ion-beam-induced transition, which is one order of magnitude lower than that obtained from thermal annealing alone (3.6 eV).[3] A large difference in the thermal activation energy was also observed between IBIEG (0.32 eV) and thermal annealing (2.7 eV) for Si.[8] The large difference was attributed to the point defects, generated from atomic collision cascades near the amorphous/crystalline interface and con-

tributing to the epitaxial growth.[8] The necessity of collision cascades near the interface to induce epitaxial growth was also confirmed in this study.[13] Therefore, similar to the silicon case, the present evidence suggests that nuclear energy loss plays a dominant role in the epitaxial transformation from amorphous to γ-alumina.

This study demonstrates that IBIEG produces better epitaxial quality γ-alumina films on sapphire at lower temperatures, as compared to conventional thermal annealing. The improved quality is indicated by the better channeling ($X_{\min}=50\%$) relative to the poorer channeling ($X_{\min}=90\%$) found in the thermally grown γ-alumina (Fig. 1). TEM results further reveal that the improved epitaxial quality produced by IBIEG is directly associated with the elimination of $\{111\}$ twins. The structural disorder associated with a high density of $\{111\}$ twin boundaries in the thermally grown γ-alumina film is the most probable reason for the high dechanneling observed in Fig. 1(b). By comparison, no distinct twin boundaries were observed in the epitaxial γ-alumina layer grown by IBIEG; any twinned boundaries as indicated by x-ray-diffraction results in Fig. 4 must have a wide spacing (>10 μm) along the interface line. However, a high density of dislocations is present in the epitaxial zone (Figs. 2 and 3). These defects are consistent with the dechanneling yield of 50% observed in Fig. 1(a). The presence of a similar level of dechanneling yields, obtained after IBIEG at 400–600 °C using Ar and O beams, suggests that these defects are not removable by IBIEG. This may be due to two effects: (1) radiation damage and (2) inherent defects in γ-alumina. The TEM results of Cao *et al.* also indicated that the γ-alumina layer formed by laser irradiation in sapphire appears to be free of twinned boundaries.[7] However, further comparison of epitaxial quality of γ-alumina formed by using these two methods is difficult due to the lack of other characterization data in Ref. 7.

The underlying mechanism for the elimination of $\{111\}$ grain boundaries in γ-alumina under ion-beam bombardment can be attributed to the ion-channeling effects. Such effects may exist in this study even at a 10° incident angle because the channeling critical angle in defected crystals is greater than that in perfect α-alumina crystals (8°). Similar effects were observed in the *in situ* ion-beam-assisted deposition (with 0.2–10-keV Ar ion beams)[14–16] and in the *ex situ* ion-beam-induced grain growth and texturing (with 10–600-keV various ion beams)[16–20] of metallic thin films. These previous studies showed that the in-plane texturing of the films is significantly improved under ion-beam bombardment either during or after thin-film deposition. The ion-channeling effects significantly reduced nuclear energy loss in the grains that aligned along the ion-beam direction. During thin-film deposition, the bombarding beam caused preferential sputtering of the nonaligned grains over the aligned grains. Therefore, only aligned grains with a large channeling spacing are favorable for growth. Similarly, under ion-beam bombardment after thin-film deposition, the nonaligned grains preferentially experience atomic collisions and energy deposition, as compared to other aligned grains. The grains which experience a higher degree of radiation damage can then undergo a structural reorientation in registry with the aligned grains during the damage recovery process. Thus, better epitaxial films can be obtained as a result of eliminating the nonaligned grains via ion-beam irradiation.[21] This study further demonstrates that the same mechanism of ion-beam bombardment is also operative for the epitaxial growth of ceramic thin films.

The orientation relationship, $[1\bar{1}0](111)\gamma \| [01\bar{1}0](0001)\alpha$, resulted from the amorphous-to-γ transition is the same for both IBIEG and thermal annealing.[5] The same orientation relationship was reported for the thermally induced amorphous-to-γ transition that occurred in ion-implantation amorphized alumina on sapphire.[2] It is of further interest to note that the α-to-γ transformation induced by Au ion irradiation[6] or by XeCl laser irradiation[7] in sapphire also produced the same epitaxial relationship. These observations support the view that the phase transitions in alumina are epitaxially related.[1,2,6,7] The small lattice mismatch ($<2\%$) between γ- and α-alumina along the close-packed direction favors the epitaxial phase transformations in the alumina/sapphire system.

The present study demonstrates that ion-beam irradiation at 400–600 °C only induces the amorphous-to-γ phase transformation. No α-alumina, epitaxial or otherwise, is observed in the grown films. It was noted that for amorphous Si on single-crystal Si,[8] thermally induced epitaxial growth starts at 450 °C ($0.43T_m$; with the melting point of Si, $T_m=1410$ °C) and IBIEG starts at 150 °C ($0.25T_m$). For thin-film alumina,[3] the thermal epitaxial growth of the γ phase and α phase starts at 650 °C ($0.4T_m$) and 950 °C ($0.52T_m$, with $T_m=2072$ °C), respectively. Referring to the Si case, the IBIEG of α-alumina should occur at $\sim$450 °C ($0.3T_m$). The absence of α-alumina suggests that ion-beam irradiation kinetically favors the formation of γ-alumina, a thermally metastable phase. Rapid cooling ($>10^{10}$ °C/sec), associated with thermal spike of ion irradiation[6] or pulsed-laser irradiation,[7] probably provides an important driving force to grow and stabilize γ-alumina. Furthermore, the study also suggests that the cubic structure may be more radiation resistant than noncubic polymorphs. This may be related to the difference in the steady-state defect density in two different phases; γ-alumina can accommodate more structural defects than α-alumina. Highly disordered γ-alumina precipitates were observed in oxygen-implanted Al.[22] A similar trend was also observed in ion-beam-irradiated sol-gel zirconia, where epitaxial cubic zirconia was formed by IBIEG at 300 °C.[23] Further examination of ion-beam-irradiation effects in amorphous alumina at higher temperatures such as 800 °C is in progress, which will provide more information regarding the phase transition and phase stability under ion-beam bombardment.

V. CONCLUSIONS

In conclusion, we have observed that ion-beam bombardment at 400–600 °C induces an amorphous-to-γ phase transformation in the amorphous alumina film deposited onto sapphire. The γ-alumina film is epitaxially related to the underlying substrate with an orientation relationship: $[1\bar{1}0](111)\gamma \| [01\bar{1}0](0001)\alpha$. Better epitaxial quality of γ-alumina ($X_{\min}=50\%$) is achieved by IBIEG than by thermal annealing alone at 800 °C ($X_{\min}=90\%$), as a result of the elimination of the $\{111\}$ twin boundaries in γ-alumina. The study also suggests that IBIEG kinetically favors the

formation of the cubic phase instead of the hexagonal phase in alumina.

ACKNOWLEDGMENTS

Useful discussions with X. D. Wu (LANL) are gratefully acknowledged. All ion-beam work was performed at the Ion Beam Materials Laboratory at Los Alamos National Laboratory. This research was sponsored by the U. S. Department of Energy, Office of Basic Energy Sciences, Division of Materials Sciences.

[1] T. C. Chou and T. G. Nieh, J. Am. Ceram. Soc. **74**, 2270 (1991).

[2] C. W. White, L. A. Boatner, P. S. Sklad, C. J. McHargue, J. Rankin, G. C. Farlow, and M. J. Aziz, Nucl. Instrum. Methods B **32**, 11 (1988); P. S. Sklad, C. J. McHargue, C. W. White, and G. C. Farlow, in *High Tech Ceramics*, edited by P. Vincenzini (Elsevier, Amsterdam, 1987), p. 1073.

[3] J. C. McCallum, T. W. Simpson, and I. V. Mitchell, Nucl. Instrum. Methods B **91**, 60 (1994).

[4] N. Yu, T. W. Simpson, P. C. McIntyre, M. Nastasi, and I. V. Mitchell, Appl. Phys. Lett. **67**, 924 (1995).

[5] N. Yu, Q. Wen, D. R. Clarke, P. C. McIntyre, H. Kung, M. Nastasi, T. W. Simpson, I. V. Mitchell, and D. Li, J. Appl. Phys. **78**, 5412 (1995).

[6] M. Ohkubo and Y. Seno, Philos. Mag. Lett. **59**, 171 (1989).

[7] S. Cao, A. J. Pedraza, D. H. Lowndes, and L. F. Allard, Appl. Phys. Lett. **65**, 2940 (1994).

[8] For a review, see F. Priolo and E. Rimini, Mater. Sci. Rep. **5**, 319 (1990).

[9] W. Zhou, D. K. Sood, R. G. Elliman, and M. C. Ridgway, Nucl. Instrum. Methods B **80/81**, 1104 (1993).

[10] N. Yu and M. Nastasi, Nucl. Instrum. Methods B (to be published).

[11] J. F. Ziegler, J. P. Biersack, and U. Littmark, *The Stopping and Range of Ions in Solids* (Pergamon, New York, 1985).

[12] F. W. Clinard, Jr. and L. W. Hobbs, in *Physics of Radiation Effects in Crystals*, edited by R. A. Johnson and A. N. Orlov (Elsevier, Amsterdam, 1986), p. 387.

[13] No crystallization was observed in a thick amorphous alumina film (200 nm) deposited on sapphire if the irradiating beam did not penetrate through the film.

[14] L. S. Yu, J. M. E. Harper, J.J. Cuomo, and D. A. Smith, Appl. Phys. Lett. **47**, 932 (1985); J. Vac. Sci. Technol. A **4**, 443 (1986).

[15] R. M. Bradley, J. M. E. Harper, and D. A. Smith, J. Appl. Phys. **60**, 4160 (1986).

[16] D. Dobrev, Thin Solid Films **92**, 41 (1982).

[17] G. N. van Wyk and H. J. Smith, Nucl. Instrum. Methods **170**, 433 (1980).

[18] P. Wang, D. A. Thompson, and W.W. Smeltzer, Nucl. Instrum. Methods B **7/8**, 97 (1985); **16**, 288 (1986).

[19] L. C. Feldman and J. W. Mayer, *Fundamentals of Surface and Thin Film Analysis* (North-Holland, New York, 1986), p. 174.

[20] J. C. Liu and J. W. Mayer, Nucl. Instrum. Methods B **19/20**, 538 (1987).

[21] M. Nastasi, J. W. Mayer, and J. K. Hirvonen, in Ion Solid Interactions: Fundamentals and Applications (Cambridge University Press, Cambridge, in press), Chap. 13.

[22] D. M. Follstaedt, S. M. Myers, and R. J. Bourcier, Nucl. Instrum. Methods B **59/60**, 909 (1991).

[23] N. Yu, P. C. McIntyre, T. E. Levine, E. P. Giannelis, J. W. Mayer, and M. Nastasi, Philos. Mag. Lett. (to be published).

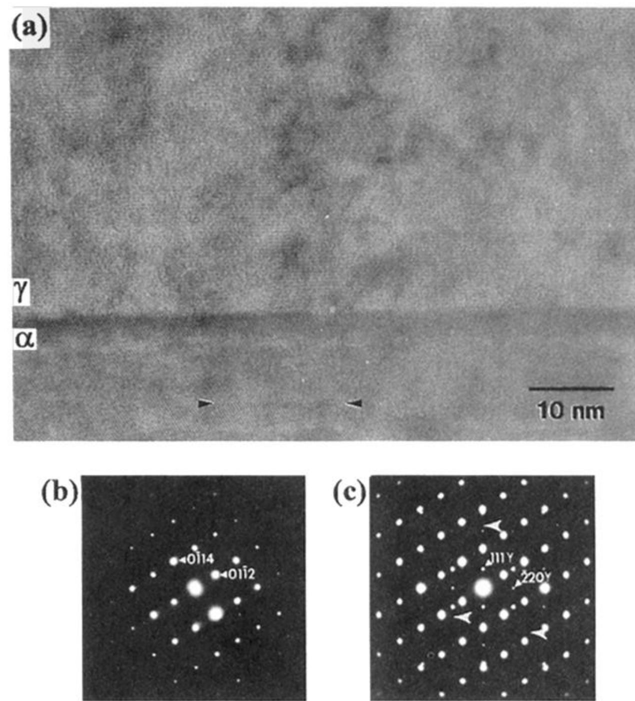

FIG. 2. (a) XTEM bright field image of the epitaxial γ-alumina/α-alumina interface; (b) SAD pattern of the α-alumina substrate; and (c) SAD pattern of both the film and substrate after irradiation with 180-keV, 6×10^{16} O/cm^2 at 500 °C.

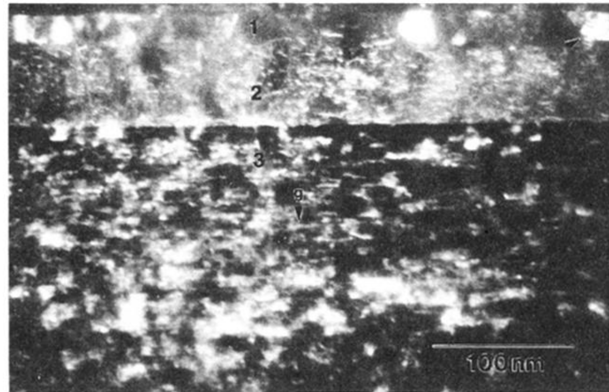

FIG. 3. XTEM weak beam image of the same specimen shown in Fig. 2; $g_{\text{film}}=[222]$ and $g_{\text{subs}}=[0006]$.